Computer Simulation of the Reentrant Cardiac Arrhythmias in Ischemic Myocardium

Hong Zhang[1,2], Lin Yang[3], Yin-bin Jin[1,2], Zhen-xi Zhang[1], and Yi-zhuo Huang[1]

[1]*Institute of Biomedical Engineering*
School of Life Science and Technology
Xi'an Jiaotong University
Shaanxi, 710049
[2]*Electric Engineering and Electronics Teaching-Experiment Center*
Xi'an Jiaotong University
Shaanxi, 710049
and
[3]*Cardiology Department, The First Hospital, Xi'an Jiaotong University*
Shaanxi, 710061, P.R. China

Abstract

Computer simulation was performed to determine how reentrant activity could occur due to the spatial heterogeneity in refractoriness induced by the regional ischemia. Two regional ischemic models were developed by decreasing the intracellular ATP concentration, reducing conductance of the inward Na^+ current and increasing the extracellular K^+ concentration on the two-dimensional sheet. Operator splitting method was used to integrate the models. The vulnerability to reentry was estimated from the timings of premature stimuli on the constructed models, which could result in unidirectionally propagating action potentials. Two kinds of sustained spiral waves and their Pseudo-Electroscardiograms were observed in numerical simulation. The results showed that the dispersion of refractory period increased with ischemic aggravation, and led to augment of the vulnerable window. A permature stimulation within the vulnerable window could easily induce spiral reentry. The Pseudo-Electrocardiograms of the spiral waves exhibited monomorphic tachycardiac waveforms. Thus, the spatial heterogeneity in refractoriness could be a substrate for reentrant ventricular tachyarrhythmias on the regional ischemic tissue.

Key Words: arrhythmia, computer simulations, ischemia, reentrant

Introduction

The most common arrhythmia observed during myocardial ischemia is ventricular tachycardia and its degeneration into fibrillation based on reentry. Dispersion of refractoriness is suggested to be the major mechanism of this arrhythmia. Specifically, it is believed that because of the inhomogeneity in the recovery of excitability, activation fronts, which are initiated by the stimulus in less refractory regions, block unidirectionally when they encounter regions of greater refractoriness, leading to reentry (4). In two dimensions a reentrant wave appears as a spiral rotation. However, it has not yet been determined how reentrant activity could occur due to this heterogenous characteristic induced by regional ischemia.

The purpose of the present study is to use a computational approach to investigate whether the spatial heterogeneity in refractoriness due to the simulated regional ischemic zone brings about reentrant tachyarrhythmias.

Materials and Methods

Mathematical Model

We constructed an excitable medium model for

Corresponding author: Dr. Hong Zhang, Institute of Biomedical Engineering, School of Life Science & Technology, Xi'an Jiaotong University, 28 West Xiannin Road, Shaanxi, Xi'an, 710049, P.R. China. Tel: 86-29-83071599, E-mail: maxr@263.net
Received: January 7, 2005; Revised: February 2, 2005; Accepted: February 10, 2005.

mammalian ventricular tissue by incorporating ordinary differential equations (ODE) into a partial differential equation (PDE) model for diffusion of the excitability. The detailed biophysical model was used as the ionic model for ventricular cell excitability. Now there are several such mathematical models available (8, 9, 10). We chose the guinea pig ventricular cell model specified by Noble, *et al*. (9) It includes concentrations of several of the ionic species Na^+, K^+ and Ca^{2+} that vary in time rather than keep fixed, internal Ca^{2+} dynamics involving Ca^{2+} uptake by and release from sarcoplasmic reticulum, and Na^+-K^+ pump and Na^+-Ca^{2+} exchange currents. The model is much more realistic in reproducing the properties of the cellular electrophysiology.

A growing body of evidence suggests that ischemia-induced action potential shortening might depend on activation of ATP-regulated potassium current, ($I_{K(ATP)}$). Therefore, in our simulation study $I_{K(ATP)}$ was added despite all the other currents specified in (9). $I_{K(ATP)}$ is inactive in healthy ventricular tissue and is increasingly outward with severity of the ischemia and decreasing levels of ATP, but it does not vary with time or voltage (10). The formulation is

$$I_{K(ATP)}=G_{K(ATP)}(V+80)/(1+([ATP]_i/0.1)^2), \quad [1]$$

where V is the transmembrane potential (mV), $[ATP]_i$ is the intracellular ATP concentration (mM), $G_{K(ATP)}$ is the maximum channel conductance per cell at $[ATP]_i$=0 mM. $G_{K(ATP)}$ was set to 0.0195 μS in our study.

Numerical Methods

Ignoring microscopic cell structure, cardiac tissue can be treated as a continuous system in which a two-dimensional sheet of isotropic ventricular muscle is modeled by the reaction-diffusion-like cable [2]

$$\partial V/\partial t=(-I_{ion})/C_m+D(\partial^2V/\partial x^2+\partial^2V/y^2), \quad [2]$$

where D is the diffusion coefficient for the transmembrane potential V, C_m is the membrane capacitance, I_{ion} is the total ionic current, t is time, x and y are spatial coordinates in the sheet. Here we chose the diffusion coefficient D=31.25 mm^2/s which could give a conduction velocity for a normal solitary plane wave along one of the coordinate axes of 400 mm/s. The canine ventricular conduction velocities range from 140-250 mm/s (transverse) to 500-800 mm/s (longitudinal), so the value of D in this study is in between the longitudinal and transverse diffusion coefficients in real anisotropic myocardium (2).

I_{ion} is a function of voltage V, gating variables Y_1, ... Y_i, ... Y_M, and ion concentrations Z_1, ... Z_i, ... Z_N. In general, the gating variables Y_i, such as m, h, d, ..., satisfy the following type of ordinary differential equation [3]:

$$dY_i/dt=a_i(1-Y_i)-\beta_iY_i \quad i=1, ..., M \quad [3]$$

where a_i and β_i are rate constants and are solely voltage-dependent. The ion concentration Z_i, such as $[Na^+]$, $[K^+]$ and $[Ca^{2+}]$, satisfy another set of ordinary differential equation [4]:

$$dZ_i/dt=f_i(I_{zi}, V, Z_i) \quad i=1, ..., N \quad [4]$$

where I_{zi} is the Z_i related ionic current.

Because of the stiffness of the partial differential equation [2], numerical integration by the conventional Euler method requires the time step to be very small during the action potential upstroke in order to keep numerical stability and accuracy. This makes the computation very time consuming. To enhance the integration efficiency, we adopted an advanced algorithm (7) to integrate equations [2] to [4]. The basic techniques of this algorithm were operator splitting and adaptive time step methods. The equations were calculated through three steps as follows.

Step 1) Using the result at time t as the initial condition to integrate the following PDE for a step length of Δt/2:

$$\partial V/\partial t=D(\partial^2V/\partial x^2+\partial^2V/\partial y^2). \quad [5]$$

Step 2) Using the result of step 1 as the initial condition to integrate the following ODE [6] and the equations [3] and [4] for a time step of Δt:

$$dV/dt=(-I_{ion})/C_m. \quad [6]$$

Step 3) Using the result of step 2 as the initial condition to integrate the PDE [5] again for a step length of Δt/2.

Practically, Step 1) and Step 3) could be combined into one step except for the first step and the last step of the whole integration epoch.

To solve the PDE [5] numerically, we used the five-point centered difference method with the impermeable boundary conditions in formula [7].

$$\partial V/\partial x|_{x=xmax,\ xmin}=\partial V/\partial y|_{y=ymax,\ ymin}=0 \quad [7]$$

The time step Δt=0.05ms was used to keep all cells synchronized. The spatial step was Δx=Δy=0.01 cm.

We integrated the ODE [6] using the second-order Runge-Kutta method with adaptive time step that was varied from minimum time step (Δt_{min}= 0.01 ms) to maximum time step (Δt_{max}=0.05 ms).

The integration by this approach was 6 times faster than the conventional Euler method, with a relative error smaller than 2%.

Numerical integration was carried out on a personal computer with a 2.8 GHz processor using programs written in visual C++. Black and white figures were constructed from these data using visual C++ program.

Simulation of Ischemia

During ischemia, the normal cell metabolism is disrupted by interruption of the O_2 supply. The results were a falling in overshoot potential and amplitude, shortening of the action potential duration, slowing of the upstroke velocity and conduction velocity, depolarizing of the resting potential, and appearing of the post-repolarization refractoriness (3).

We developed two ischemic models in our study by changing the physiological variables. They involved the fall in intracellular ATP concentration (ATP_i), the decrease in inward Na^+ conductance (G_{Na}) and the increase in extracellular K^+ concentration ($[K^+]_o$). These parameters were combined together to simulate different severity of the ischemia referred to as the moderate and severe ischemia in Table 1.

Regional Ischemia

The simulation was conducted on a two-dimensional matrix consisting of 200×200 elements. The length of each element was set to be 100 μm. Thus the thin-sliced square section of the ventricular myocardium corresponded to 20 mm×20 mm. Each element was assumed to be a cluster of homogeneous myocardial cells, and was electrically coupled with four immediate neighbors by gap junctions.

The simulated regional ischemic zone was introduced into the healthy tissue. The transition from normal to abnormal tissue was sudden with an abrupt change, but electrophysiological properties of the cells contained in one certain ischemic zone were assumed to be same.

Measurement of the Vulnerable Window and Initiation of Spiral Wave

The vulnerable window was determined by the extrastimulus technique. After the stimulus S1, an early extrastimulus S2 was introduced. All stimuli were applied from the left half of the top border of the matrix with 12 μA/μF in amplitude and 2 ms in duration for each element.

We defined the limits of the vulnerable window as the lowest and highest values of the S1 S2 interval for which the unidirectional propagation could be initiated. Initiation of spiral waves was defined as the successful reactivation of the whole matrix after the wave front of S2 activated the whole matrix.

Table 1. Model parameters for three types of cells

Type	Parameters		
	ATP_i (mM)	G_{Na} (μS)	$[K^+]_o$ (mM)
Normal	6.5	2.5	4.5
Moderate ischemia	2.0	1.75	8.5
Severe ischemia	0.7	0.85	13.0

*ATP_i is the intracellular ATP concentration, G_{Na} is the inward Na^+ conductance, and $[K^+]_o$ is the extracellular K^+ concentration.

Pseudo-Electrocardiogram (pseudo-ECG)

We calculated the measurable electrical activity as a Pseudo-Electrocardiogram to display the properties of spiral wave propagation. The way to calculate the pseudo-ECG is by subtracting the average potential in the upper half of the tissue from the average potential in the lower half of the tissue by the following equation (6, 11):

$$ECG = \frac{1}{20000}\left(\sum_{i=1}^{i=200}\sum_{j=1}^{j=100} V_{i,j} - \sum_{i=1}^{i=200}\sum_{j=101}^{j=200} V_{i,j}\right). \quad [8]$$

Results

Characteristics of the Simulated Cells

We measured properties of the constructed single cell models shown in Tab.1 and their action potentials. The APD90 (the time taken for a cell to repolarize to 90% of the amplitude of action potential) of the normal, moderate and severe ischemia were 122 ms, 71 ms and 48 ms, respectively. Their maximum membrane rates of depolarization were 380 V/s, 320 V/s and 198 V/s. Resting potentials were -89 mV, -73 mV and -63 mV.

The simulated ischemic cell was characterized by obvious reduction in APD, slower APD upstroke, and less negative resting potential, just as observed during the experiment (3). Moreover, ischemic cells exhibited post-repolarization refractoriness. In contrast, during ischemia the refractory (absolute and relative) period prolonged despite shortening of the APD and could outlast full repolarization by tens or even hundreds of milliseconds. The more severe the ischemia was, the longer the refractory period was. However, the normal cell did not have this property.

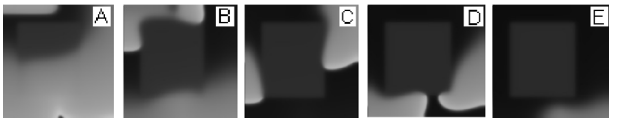

Fig. 1 Wave propagated in two directions when the S1 S2 interval was greater than the upper limit. Snapshots A to E were taken after the start of the S2 simulation: 5 ms, 35 ms, 70 ms, 150 ms and 180 ms, respectively. Brightness shows membrane voltage with darker regions showing resting tissue (V_m = -90 mV) and lighter regions depolarized tissue (V_m = 50 mV).

Therefore, the dispersion of refractory period between normal and ischemic tissue was increased with aggravation of the ischemia.

Vulnerable Window

We measured the vulnerable window which could induce unidirectional propagation and cause spiral waves. When the S1 S2 interval was smaller than the lower limit, the stimulus was completely blocked. When the interval was higher than the upper limit, the stimulus could propagate in two directions, collided with each other and disappeared finally (Fig. 1). Only when the S2 stimulus was within the vulnerable window could the spiral wave be initiated. The vulnerable windows were 6 ms and 17 ms for moderate and severe regional ischemia, respectively, and less than 1ms for the normal homogeneous tissue. These results indicated that the vulnerable window increased with the higher level of refractory dispersion.

Sustained Spiral Wave

Sustained spiral waves were observed on the regional ischemic tissue except for the homogeneous normal tissue. Two patterns of the activation behavior were observed. One was on the regional moderate ischemia (Fig. 2). Another was on the regional severe ischemia (Fig. 3). In both cases, refractory periods of the simulated ischemic tissues were much longer than those of the normal tissues, even though they had returned to the resting potential due to appearance of post-repolarization refractoriness. The ischemic regions were clearly visible in the whole tissues due to raised resting potential and the plane waves were slowed in these regions.

In Fig. 2, when S2 stimulus was exerted during the vulnerable window, activation wave front could propagate in one direction (snapshot A). Since the simulated moderately ischemic region was still refractory, the wave moved along the border between normal and ischemic region (snapshot B). With the excitation recovery of the ischemic region, the

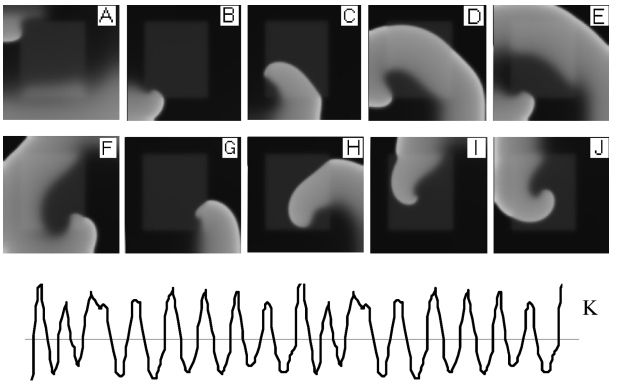

Fig. 2 Sustained spiral wave and its pseudo-EGG (K) in the regional moderately ischemic tissue. Snapshots A to J were taken after the start of the S2 simulation: 25 ms, 70 ms, 90 ms, 110 ms, 120 ms, 135 ms, 160 ms, 180 ms, 270 ms and 280 ms, respectively.

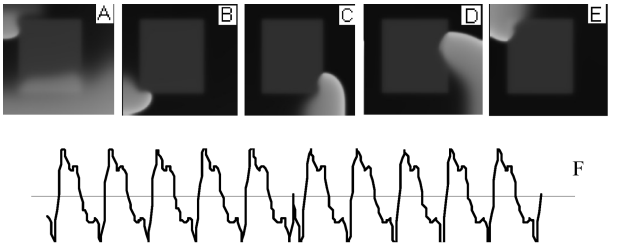

Fig. 3 Sustained spiral wave and its pseudo-EGG (F) in the regional severely ischemic tissue. Snapshots A to E were taken after the start of the S2 simulation: 25 ms, 70 ms, 110 ms, 130 ms and 180 ms, respectively.

activation wave spread across the whole tissue (snapshots C to F). After that the ischemic region again became unexcitable and the wave moved along the border (snapshot G) until the ischemic region once more got excited (snapshots H to J). The reentry wave could sustain 4 minutes until the experiment ended. The wave of this type approximately exhibited a monomorphic waveform similar to ventricular tachyarrhythmias (VT) on the Pseudo-ECG (K); however, slight meandering of the tip of the spiral wave resulted in a small difference in the amplitude between the complexes.

The behavior of reentry in Fig. 3 was, however, different. Since excitability of the simulated severely ischemic region was much lower, it became a block region. The reentry wave front as a source could not activate this large sink. The spiral reentry could no longer be induced in the ischemic region in this case. Thus the reentrant wave tended to move along the border between simulated normal and ischemic region until the end of the experiment (snapshots A to E). The Pseudo-ECG (F) of this type also displayed a

monomorphic waveform similar to VT. However, because of the effects of the severe ischemia, the velocity of the reentrant wave was greatly slowed down. Thus, the frequency of the ECG in this type was smaller than that in the former one. Moreover, the amplitude of the ECG in this type was much more consistent between the complexes. This implied that the reentrant wave on the regional severe ischemia was more stable than it was on the moderate ischemia.

Discussion

The ionic model based on myocardial ionic dynamics was used in our simulation study. The model could better approximate the real dynamics of myocardial ionic currents, thus becoming more accurate in studying mechanisms of cardiac arrhythmias. Shapes and properties of the action potentials in our simulated normal and ischemic models were proved to be in good agreement with others (5).

It was reported that reentry was more common in hearts with structural and/or functional abnormalities such as ischemia. The spatial heterogeneity in refractoriness was suggested as a substrate (3). To evaluate this assumption, the moderately and severely ischemic models were introduced into the two-dimensional tissues. Although the abrupt change between normal and ischemic border, which was the case in our simulation, might not represent an actual condition, such a simple spatial heterogeneity enabled us to clearly observe the basic relationship between the dispersion of refractory period and the activation propagation behavior.

The double sequential stimulation from a single source was used as an eligible method. The stimulation site located on the left half of the top border of the constructed tissue for an asymmetrical collision that was much closer to reality.

The vulnerable windows were measured on our constructed tissues. The window became wider as the level of dispersion in refractoriness became higher. These results were consistent with other reports (1, 11).

Two sustained spiral waves were observed in our models. On the regional moderately ischemic tissue, the ischemic zone could be activated although its refractory period was longer than that in the normal tissue. The tip of the spiral wave meandered a lot that made amplitude of its Pseudo-ECG different from time to time, but it still resembled the VT rather than the torsades de pointes (TdP). On the regional severely ischemic tissue, the reentrant wave front could not activate the ischemic zone and tended to move along the border between simulated normal and ischemic regions. The Pseudo-ECG exhibited much more stable characteristics with lower frequency.

Our major findings suggested that a premature stimulation within the vulnerable window could easily induce spiral reentry. The width of the vulnerable window was increased with aggravation of the ischemia. Thus, the spatial heterogeneity in refractoriness could be a substrate for reentrant tachyarrhythmias on the regional ischemic tissue.

Acknowledgment

This work was supported by National Natural Science Foundation of P.R. China 60378018, 30100067 and the Doctoral Foundation of Xi'an Jiaotong University DFXJTU 2003-12, Xi'an, P.R. China.

References

1. Akar, F.G. and Rosenbaum, D.S. Transmural electrophysiological heterogeneities underlying arrhythmogenesis in heart failure. *Circ. Res*. 93: 638-645, 2003.
2. Biktashev, V.N. and Holden, A.V. Re-entrant waves and their elimination in a model of mammalian ventricular tissue. *Chaos* 8: 48-56, 1998.
3. Carmeliet, E. Cardiac ionic currents and acute ischemia: from channels to arrhythmias. *Physiol. Rev*. 79: 917-1017, 1999.
4. Cascio, W.E. Myocardial ischemia: What factors determine arrhythmogenesis? *J. Cardiovasc. Electrophysiol*. 12: 726-729, 2001.
5. Clayton, R.H., Parkinson, K. and Holden, A.V. Re-entry in computer models of ischaemic myocardium. *Chaos Solitons Fractals* 13: 1671-1683, 2002.
6. Davidenko, J.M., Salomonsz, R. and Pertsov, A.M. Effects of pacing on stationary reentrant activity: Theoretical and experimental study. *Circ. Res.* 77: 1166-1179, 1995.
7. Jin, Y.B., Yang, L., Zhang, H., Kuo, Y.H., Huang, Y.Z. and Jiang, D.Z. Numerical algorithm for conduction of action potential in two-dimensional cardiac ventricular tissue, (in Chinese). *J. of Xi'an Jiaotong Univ.* 38: 851-854, 2004.
8. Luo, C.H. and Rudy, Y. A dynamic model of the cardiac ventricular action potential. I. Simulations of ionic currents and concentration changes. *Circ. Res.* 74: 1071-1096, 1994.
9. Noble, D., Noble, S.J., Bett, G.C., Earm, Y.E. and Ho, W.K. The role of sodium-calcium exchange during the cardiac action potential. *Ann. NY. Acad. Sci.* 639: 334-353, 1991.
10. Noble, D., Varghese, A., Kohl, P. and Noble, P. Improved guinea-pig ventricular cell model incorporating a diadic space, Ikr and Iks, and length- and tension-dependent processes. *Can. J. Cardiol.* 14: 123-134, 1998.
11. Tsunetoyo, N., Takashi, A., Kazuo, N. and Tohru, O. Spatial heterogeneity in refractoriness as a proarrythmic substrate: Theoretical evaluation by numerical simulation. *Jpn. Circ. J.* 64: 121-129, 2000.